



Preparation of Ag/ZnO microspheres and study of their photocatalytic effect on dichloromethane

Zhibing Xu, Nian Liu, Yi Han*, Pengfei Zhang, Zhiming Hong, Jingcheng Li

College of Resources and Environment, Anqing Normal University, Anhui 246011, China, emails: yihan@whu.edu.cn (Y. Han), xuzhibing@163.com (Z. Xu), 1977511845@qq.com (N. Liu), 601653169@qq.com (P. Zhang), 1303599733@qq.com (Z. Hong), 1210530870@qq.com (J. Li)

Received 29 April 2020; Accepted 20 November 2020

ABSTRACT

Carbon microspheres were successfully synthesized using glucose, urea, and zinc salt as raw materials at low temperatures. Carbon microspheres were soaked in silver nitrate solution and calcined at 500°C for 3 h to obtain Ag/ZnO microspheres. The samples obtained were characterized using X-ray diffraction, scanning electron microscopy, and energy-dispersive X-ray spectroscopy. Dichloromethane degradation was investigated under visible light by using Ag/ZnO microspheres as photocatalysts. Results showed that the Ag/ZnO-3 microspheres had improved photocatalytic effects on dichloromethane. Ion chromatography and conductivity methods were used to measure the varied photocatalytic time data of dichloromethane solution, and their results were compared. The conductivity of the dichloromethane solution increased from 14 to 32 $\mu\text{S cm}^{-1}$ after photocatalysis for 180 min with Ag/ZnO-3 microspheres. $\cdot\text{OH}$ played a major role in the degradation process, and the steady-state concentration of $\cdot\text{OH}$ was $1.54 \times 10^{-15} \text{ mol L}^{-1}$ in the composite microspheres was prepared by soaking with 0.05 M Ag photocatalyst. Liquid chromatography was used to analyze the valid photocatalytic reaction time of the liquid chromatogram. Results suggested that in the photocatalytic reaction, dichloromethane was dechlorinated into carbon dioxide and hydrogen chloride.

Keywords: Ag/ZnO microspheres; Photocatalysis; Dichloromethane

1. Introduction

As a common pollutant in drinking water, dichloromethane (CH_2Cl_2) usually comes from industrial pollution or harmful components from the chlorination of water [1,2]. Dichloromethane contributes to the pollution of soil, water bodies, and air; the decay of the stratospheric ozone layer; and smog formation and generates harmful odors, leading to chronic toxicity in humans, animals, and vegetation [3–6]. Therefore, dichloromethane is an important indicator, and waterworks must be monitored. CH_2Cl_2 should be eliminated before discarding the wastewater into the environment.

Photocatalysts have attracted a lot of attention in energy conversion and pollution purification in recent years. Among various photocatalysts, semiconductor photocatalysts are one of the best choices because of their good stabilities, adjustable band gaps, and high activity [7–10]. ZnO nanoparticles are widely used as traditional functional materials in solar energy, catalysts, medicine, and cosmetic substances. Substantial research is devoted to the preparation and the performance of ZnO nanoparticles and their compounds and the preparation of different kinds of morphological ZnO nanoparticles and their compounds [11–15]. Compared with particle materials, ZnO nanoparticles

* Corresponding author.

and their compounds have gained considerable attention because of their special structure, specific surface area, and a wide range of applicability [16–18]. Aside from the structural design, the decoration of a noble metal can improve the photocatalytic activity of conventional photocatalysts [19,20]. The Ag nanoparticles in Ag/ZnO compounds are the key to enhance the catalytic performance [21–24]. Ag has attracted attention due to its low cost, nontoxicity, and high electrical and thermal conductivities. A series of Ag/ZnO nanocomposites with different morphologies (such as nanoparticles, nanofiber, hollow microspheres, microrods, and cauliflower- and pom-pom-, dendrite-, and flower-like ZnO microstructures [25–31]) is prepared through various methods. Moreover, these composites have received much attraction in many photofunctional applications including solar cell, photocatalytic water splitting, purification of water and air, and bacterial inactivation [32].

Herein, we present a facile and practical method to fabricate new structural Ag/ZnO compounds. In accordance with previous studies and experiments, the carbon microspheres are synthesized using glucose, urea, and zinc nitrate in an autoclave at low temperature [33]. Carbon microspheres serve as templates to prepare ZnO and Ag/ZnO microspheres. The effects of Ag content on the structural properties of ZnO are studied. In addition, the morphologies, structures, and photoelectric properties of Ag/ZnO nanocomposites are investigated. The photoactivity of the prepared nanocomposites is assessed based on the dichloromethane photodegradation.

2. Experimental

2.1. Experimental material

Glucose ($C_6H_{12}O_6 \cdot H_2O$, analytically pure), zinc nitrate ($Zn[NO_3]_2 \cdot 6H_2O$, 99.0%, analytically pure), silver nitrate ($AgNO_3$, 99.8%, analytically pure), dichloromethane (CH_2Cl_2 , 99.5%), and urea ($CO[NH_2]_2$, 99.0%, chemically pure) were purchased from Sinopharm-China. All reagents were used without further purification. Deionized water was used throughout this study.

2.2. Preparation of ZnO and Ag/ZnO microsphere photocatalysts

Initially, 6.0 g glucose and 1.0 g urea were added to 40 mL deionized water. The mixture was stirred for 10 min, added with 2.0 g zinc nitrate, and stirred for 10 min. The solution was hydrothermally treated in Teflon-line autoclave (50 mL) at 135°C and 150°C subsequently for 3 h each. The solution was kept at room temperature, and the black precipitate was filtered. The product was rinsed thoroughly with deionized water and dried at 80°C for 5 h, and carbon microspheres were obtained.

The impregnation method was used to prepare Ag/ZnO microspheres. The prepared carbon microspheres (2.0 g) were immersed in 20 mL silver nitrate solution for 2 h, and the concentrations of the silver nitrate solution were 0.005, 0.025, 0.05, and 0.1 M. After drying at 80°C, carbon microspheres were placed in a muffle furnace at 500°C for 3 h. Finally, Ag/ZnO microspheres were obtained through the calcination of carbon microspheres and kept

at room temperature. Samples were labeled as Ag/ZnO-1, Ag/ZnO-2, Ag/ZnO-3, and Ag/ZnO-4.

2.3. Characterization of Ag/ZnO microspheres

The powder X-ray diffraction (XRD) was carried out using the XRD-6000 (SHIMADZU, Japan) with the copper target, and the $K\alpha$ radiation was used for the phase identification. Diffracted X-ray intensities were recorded as a function of 2θ . Scanning electron microscopy (SEM) was conducted using the S-4700 (Hitachi, Japan) instrument and the LED 1530VP SEM. Energy-dispersive X-ray spectroscopy (EDS) was performed using the OXFORD EDS(UK). The specific surface areas and the pore structures of the samples were determined using a nitrogen adsorption apparatus (BELSORPmini, BEL, Japan). The elements of each sample were determined through ICP-OES measurements (Agilent 720-ES instrument, USA), and the samples were digested in a mixture of sulfuric and nitric acids. The bandgap of Ag/ZnO microspheres were analyzed via UV-vis absorption using PE lambda 750S (USA) in the spectral range 300 to 700 nm.

2.4. Measurement of the photocatalytic activity

Dichloromethane (CH_2Cl_2) was used as a model organic compound to investigate the photocatalytic activity of Ag/ZnO microspheres. The catalyst (25 mg) and CH_2Cl_2 (0.1 mL) were added into 50 mL purified water, and the mixture was stirred in the dark. The conductivity of the chloride ion concentration in the CH_2Cl_2 solution was tested. The solution was stirred under irradiation of two 36 W fluorescent lamps, and the conductivity of the chloride ion concentration was tested every 30 min. The effect of the CH_2Cl_2 photocatalytic dechlorination was analyzed through the changes in the conductivity of the chloride ion concentration in the dichloromethane solution. Ion chromatography (IC) was conducted using the DIONEX ICS-100, whereas liquid chromatography (LC) was conducted using the SHIMADZU LC-10Atvp, SPD-10Avp ultraviolet-visible photometric detector, Rheo-dyne 7725 sample valve, and Chiang's chromatography workstation (using C18 chromatogram column).

2.5. Determination of the free radical ($\cdot OH$) concentration

The concentration of hydroxyl radicals ($\cdot OH$) is an essential factor in the photocatalytic process and has a positive relationship with the oxidation ability. The salicylic acid method was used to determine the concentration of $\cdot OH$. The theoretical basis for this method was that salicylic acid captured $\cdot OH$ to generate 2,3-dihydroxy benzoic and 2,5-dihydroxy benzoic. The reactants had a maximum optical absorption peak at 510 nm. The type 722 spectrophotometer, which was purchased from Shanghai Precision Scientific Instrument Co., Ltd. (China), was used to determine the $\cdot OH$ concentration.

The concentration of hydroxyl radicals was calculated in accordance with Eq. (1):

$$[\cdot OH]_{-ss} = \frac{K_c}{K_B} \quad (1)$$

where $[\cdot\text{OH}]_{\text{ss}}$ is the steady-state $\cdot\text{OH}$ concentration in $10^{-15} \text{ mol L}^{-1}$, K_p is the pseudo-first-order reaction rate constant in s^{-1} , and K_B is the second-order rate constant ($2.7 \times 10^{10} \text{ mol}^{-1} \text{ L s}^{-1}$) [34].

3. Results and discussion

3.1. Photocatalytic activity of Ag/ZnO microspheres

The photocatalytic activity of Ag/ZnO microspheres was conducted using two 36 W fluorescent lamps as the irradiation source. The catalyst (25 mg) was added to the dichloromethane solution for a photocatalytic reaction. The changes in the conductivity of the solution under varied photocatalytic times in the photocatalytic process are shown in Fig. 1.

Fig. 1 shows the changes in the solution conductivity of the photocatalytic reaction under the effect of Ag/ZnO series catalysts. When Ag/ZnO microsphere photocatalysts were added into the dichloromethane solution, the dichloromethane degradation improved evidently. Among the Ag/ZnO catalysts, Ag/ZnO-3 exhibited the most ideal catalytic effect. The dichloromethane solution conductivity increased from 14 to $32 \mu\text{S cm}^{-1}$ after photocatalysis for 180 min. At low Ag content, the photocatalytic performance of ZnO was not promoted. However, the excess Ag was deposited on the surface of ZnO, which hindered the photocatalytic reaction. This phenomenon reduced the photocatalytic activity of the catalyst, which mainly due to the addition of Ag beyond the optimum concentration will decrease the degradation rate due to the excess Ag on ZnO surface blocking UV light [35].

Additionally, IC was used to measure the chloride ion concentration at various time points, such as before adding catalysts, adsorption in the dark for 30 min, and varied times of photocatalysis by using Ag/ZnO-3 microspheres as catalysts. This step was done to determine the conductivity

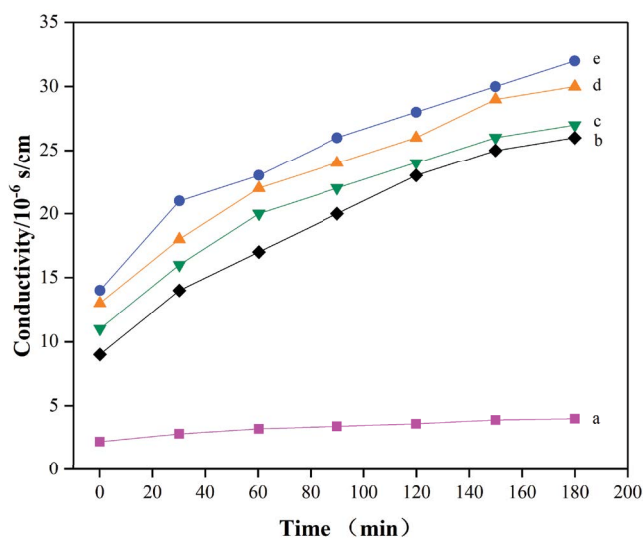


Fig. 1. Effect of Ag/ZnO microspheres on dichloromethane (a) without catalyst, (b) Ag/ZnO-1, (c) Ag/ZnO-2, (d) Ag/ZnO-4, and (e) Ag/ZnO-3.

of the dichloromethane solution and investigate whether it could reflect the photocatalytic degradation of dichloromethane. The chloride ion concentration and the conductivity of the dichloromethane solution at varied time points are shown in Table 1.

The electrical conductivity and the chloride ion concentration of the dichloromethane solution of the experimental and the control groups were compared. The change in the conductivity of dichloromethane in the aqueous solution was consistent with the change in chloride ion concentration ($R^2 = 0.9065$, $P < 0.05$), and the photocatalytic dechlorination effect of dichloromethane in water could be better reflected by measuring the conductivity of the aqueous solution.

3.2. Photocatalytic mechanism

3.2.1. XRD pattern of Ag/ZnO-3 microspheres

The XRD patterns of Ag/ZnO-3 are presented in Fig. 2. The sample diffraction peaks at 31.9° , 34.6° , 36.4° , 47.7° , 56.8° , 63.1° , 66.6° , 68.2° , and 69.3° were consistent with the peaks of ZnO [36], whereas the peaks at 38.1° , 44.3° , and 64.5° were consistent with the peaks of Ag [37]. This result suggested that the high-temperature roasted samples were compounds of Ag/ZnO.

Table 1

Comparison of two methods for the determination of dichloromethane solution

Time (min)	Ion chromatography (mg/L)	Conductivity ($\mu\text{S/cm}$)
Before absorption	0.07	2.0
After absorption	0.11	14
30	0.18	21
60	0.35	23
90	0.48	26
120	0.56	28
150	0.61	30
180	0.64	32

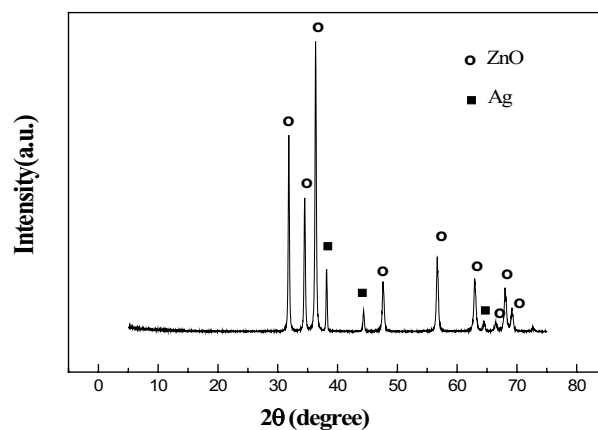


Fig. 2. XRD pattern of Ag/ZnO-3 microspheres.

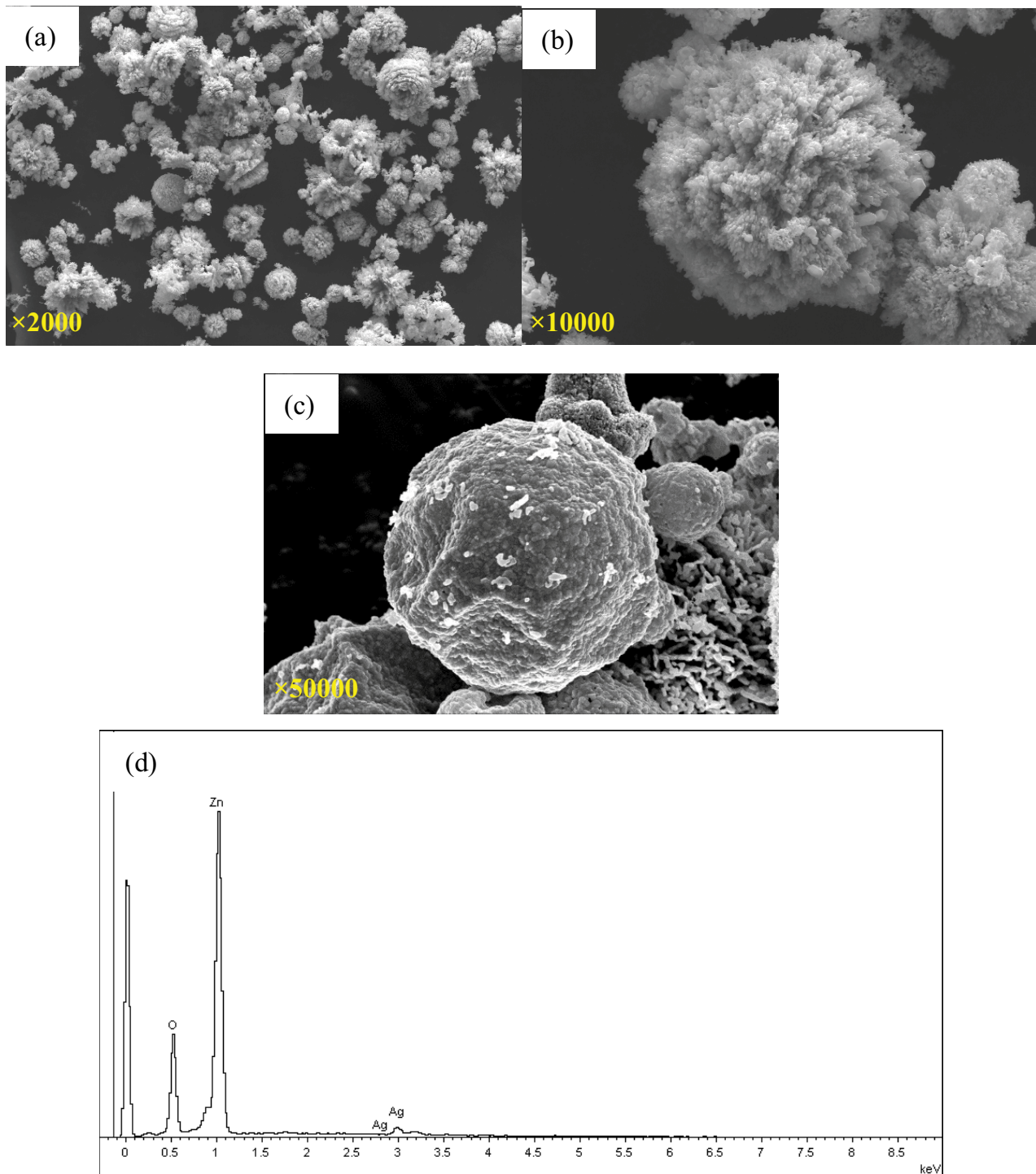


Fig. 3. SEM images of (a and b) Ag/ZnO-3, (c) ZnO microspheres, and EDS spectrum (d) Ag/ZnO-3 microspheres.

3.2.2. SEM and EDS of Ag/ZnO-3 microspheres

Figs. 3a and b show the SEM images of the overall appearance and the surface structure of Ag/ZnO-3 microspheres. The diameters of Ag/ZnO-3 microspheres ranged from 8 to 15 μm . An SEM image of ZnO (c) alone has been given, it could be found that the diameters of the Ag/ZnO-3

microspheres were larger than those of ZnO. The microspheres comprised ZnO particles and silver nanoparticles, the overall structures were loose. The microsphere structure could present a superior performance in the photocatalytic reaction because of their low density, high surface area, easy settlement, good delivering ability, and surface permeability [24,38,39].

The EDS method was used to analyze the presence of Ag in the prepared ZnO microsphere. The spectrum showed that the surface of Ag/ZnO-3 microspheres had Ag, Zn, and O elements without impurities (Fig. 3d).

3.2.3. Specific surface area of Ag/ZnO microspheres

The nitrogen adsorption and desorption of Ag/ZnO-1, Ag/ZnO-2, Ag/ZnO-3, and Ag/ZnO-4 samples obtained using high-temperature roasting were studied. The BET specific surface areas of each sample are shown in Table 2. Results showed that with increasing amount of Ag added in the preparation process, the specific surface area of Ag/ZnO microspheres prepared using high-temperature roasting decreased gradually. When the concentration of AgNO₃ increased from 0.005 to 0.05 M for Ag/ZnO microsphere preparation, the specific surface area decreased to 2.48 m² g⁻¹. Further increase sharply reduced the specific surface area, which may lead to the poor photocatalytic activity of the catalyst, and this finding was consistent with the degradation results.

3.2.4. Elemental analysis of Ag/ZnO microspheres

The chemical compositions of Ag/ZnO-1, Ag/ZnO-2, Ag/ZnO-3, and Ag/ZnO-4 samples were analyzed using ICP-OES. The ICP-OES results of the elements of each sample are summarized in Table 3.

In Table 3, when the initial concentration of AgNO₃ increased from 0.005 to 0.1 M for Ag/ZnO microsphere preparation, the mass fraction of Ag in Ag/ZnO increased from 2.4% to 34.03%, and the optimum content of Ag in Ag/ZnO composite was 17.73%.

3.2.5. Optical property

The bandgap energy of semiconductor-based photocatalyst material plays a dynamic role in deciding the

photocatalytic activity under light irradiation [40]. The Ag/ZnO-3 microsphere was analyzed via UV-vis absorption, the photoluminescence spectra (PL) of Ag/ZnO-3 microsphere is shown in Fig. 4. From the raw data obtained in UV-vis absorption, the band-gap is calculated using Tauc's formula [39], as shown in Eq. (2). The band-gap of Ag/ZnO-3 microsphere comes out to be approximately 2.89 eV, lower than the band-gap of ZnO, which is favorable for improved photocatalytic activity due to modification in bandgap energy [11]. Moreover, ZnO photocatalyst modified by Ag will improve its photocatalytic activity and impose the photostability of ZnO [41,42].

$$(\alpha h\nu)^2 = h\nu - E_g \quad (2)$$

wherein α , h , and ν represented absorption coefficient, Planck constant, and light frequency, respectively [43].

3.2.6. Free radical (*OH) concentration

Hydroxyl radical (*OH) was generated during photocatalysis, which plays a leading role for the removal of resistant organic pollutants from water [11,19]. The catalytic performance of microspheres could be evaluated by determining the concentration of *OH. In this study, the salicylic acid method was used to determine the concentration of *OH. Results are shown in Fig. 5. The absorbance of experimental groups increased with time. The group soaked with 0.05 M Ag showed the largest increase, suggesting that the production of *OH was more than that of the other groups. Large amounts of *OH could effectively oxidize the pollutants in water, which was consistent with the experimental results above.

In accordance with the formula $[*OH]_{ss} = K_i/K_B$ [44], the experimental results were obtained (Table 4). After 60 min of photocatalysis, the steady-state concentration of *OH could be concluded as 1.54×10^{-15} mol L⁻¹ in the composite microspheres prepared by soaking with 0.05 M Ag photocatalyst, and this value was higher than those in

Table 2
Surface area data for Ag/ZnO microspheres

Sample	S_{BET} (m ² /g)
Ag/ZnO-1	5.36
Ag/ZnO-2	2.56
Ag/ZnO-3	2.48
Ag/ZnO-4	0.72

Table 3
ICP-OES results for Ag/ZnO microspheres

Sample	Ag (%)	Zn (%)
Ag/ZnO-1	2.4	79.19
Ag/ZnO-2	9.73	71.48
Ag/ZnO-3	17.73	66.14
Ag/ZnO-4	34.03	52.62

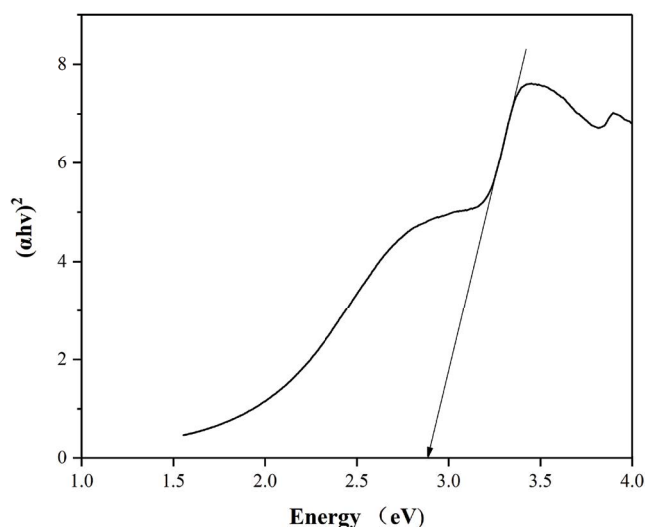


Fig. 4. Tauc's plot for Ag/ZnO-3 microsphere.

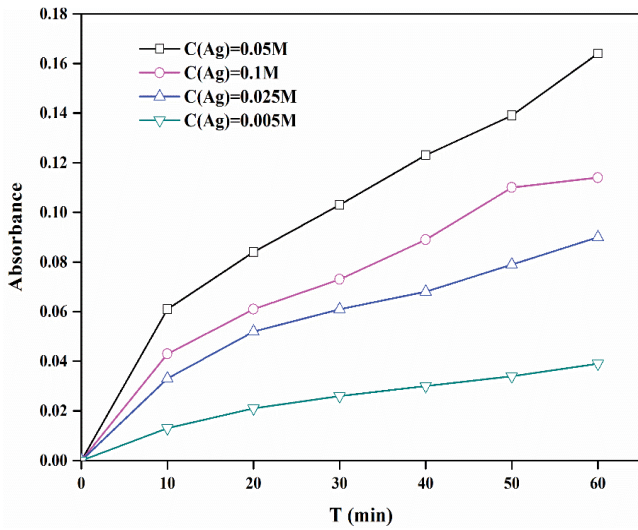


Fig. 5. Absorbancy of $\cdot\text{OH}$ concentration with different Ag/ZnO Catalyst.

other composite microspheres. Therefore, for the composite microspheres prepared by soaking with different concentrations of Ag, when the concentration of Ag was 0.05 M, increased $\cdot\text{OH}$ could be produced in the photocatalytic process of the prepared composite microspheres.

3.2.7. Analysis of the degradation process

LC was used to analyze the dichloromethane solution after 1 and 4 h of photocatalytic reaction by using Ag/ZnO-3 microspheres as catalysts. The mobile phase of the liquid chromatograph comprised methyl alcohol and water (volume ratio of 55:45). The flow rate was 1 mL min^{-1} , and the determined wavelength was 218 nm. The liquid chromatogram of the dichloromethane solution after photocatalysis for 1 and 4 h are shown in Fig. 6.

The liquid chromatograms of the dichloromethane photocatalytic degradation after 1 and 4 h were compared in the figures above. The dichloromethane solution after 1 h of photocatalysis still showed undecomposed dichloromethane chromatographic peaks (retention time is 5.208 min).

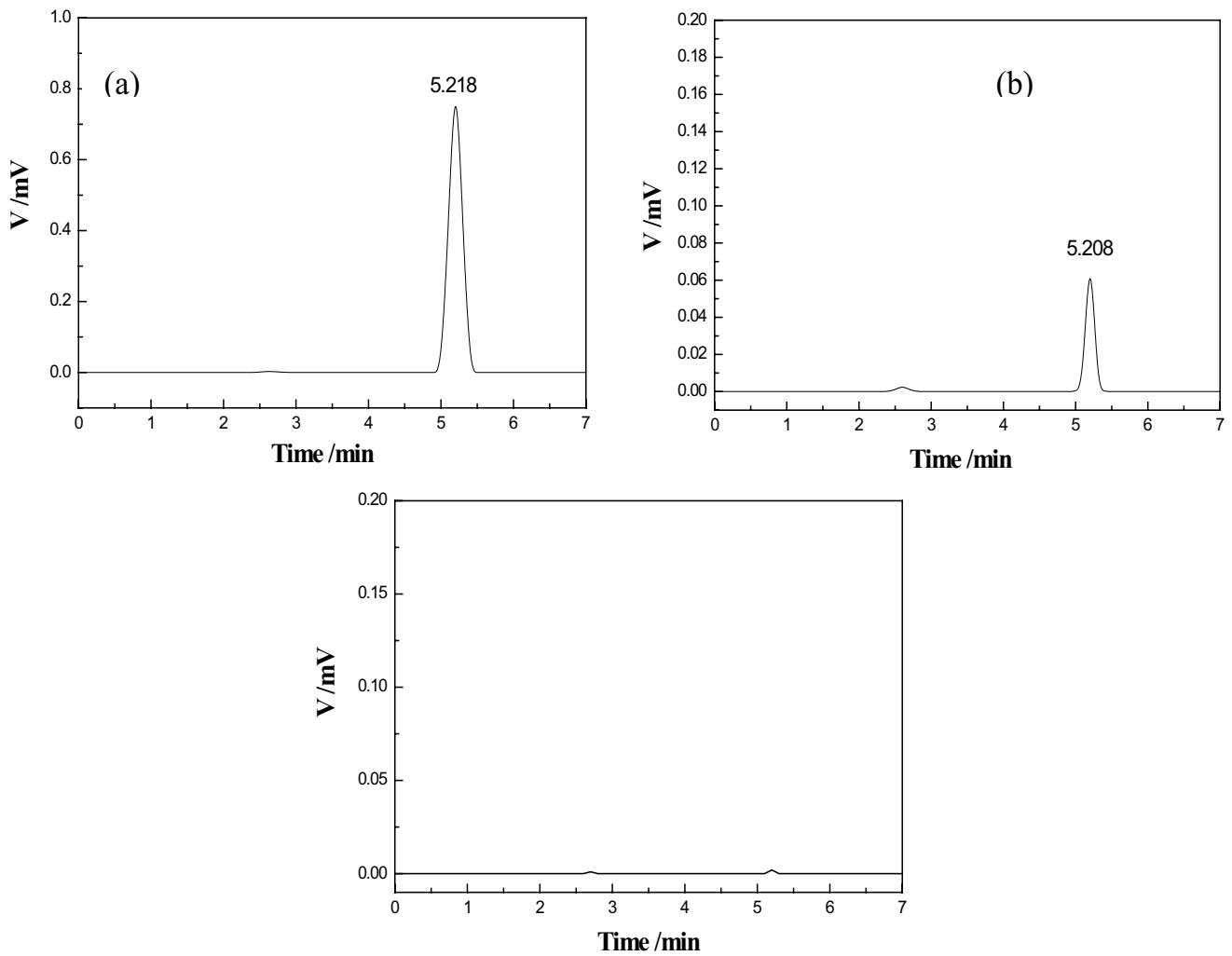


Fig. 6. Liquid chromatogram of dichloromethane solution (a) control, (b) after photocatalysis for 1 h, and (c) after photocatalysis for 4 h.

Table 4
Radical concentration of different Ag/ZnO microspheres

C (Ag) (mol/L)	n (sample points)	R ²	K _c (10 ⁻³ min ⁻¹)	[•OH] _{ss} (10 ⁻¹⁵ mol/L)
0.1	6	0.9434	1.8	1.11
0.05	6	0.9451	2.5	1.54
0.025	6	0.9239	1.4	0.86
0.005	6	0.9443	0.6	0.37

After 8 h of photocatalytic process, the solution showed no dichloromethane chromatographic peak and other mid-decomposition products. This result suggested that dichloromethane was decomposed into carbon dioxide and hydrogen chloride directly through photocatalysis.

3.2.8. Photocatalytic mechanism summary

The response ability of composite microspheres to visible light was enhanced due to the Ag particles attached to the surface of microspheres. Ag/ZnO microspheres can adsorb more dichloromethane molecules because of their large specific surface area, thereby promoting the reaction between dichloromethane molecules and hydroxyl radicals in the system. The electrons of Ag/ZnO microspheres were transferred from the valence band to the conduction band by absorbing photons, and positively charged holes were formed in the valence band at the same time. Then, •OH was produced with the reaction between H₂O molecules and holes, and dichloromethane was decomposed into CO₂, H⁺, and Cl⁻ with the oxidation of •OH (Fig. 7). Ag is considered as one of most promising photocatalysts for the oxygen reduction reaction [45], indicating that photogenerated electrons can reduce O₂ into the superoxide radical easily on the Ag particles in the photocatalytic progress [46,26]. More superoxide radicals are generated, enhancing the photocatalytic activity.

4. Conclusion

Doping appropriate Ag onto the Ag/ZnO microspheres is effective in improving the photocatalytic performance. The effect of the catalyst on dichloromethane can be analyzed using the conductivity of the dichloromethane solution. The conductivity increased from 14 to 32 μs cm⁻¹ after photocatalysis with Ag/ZnO-3 microspheres for 180 min. •OH was proven to play a major role in the degradation process, and the steady-state concentration of •OH was

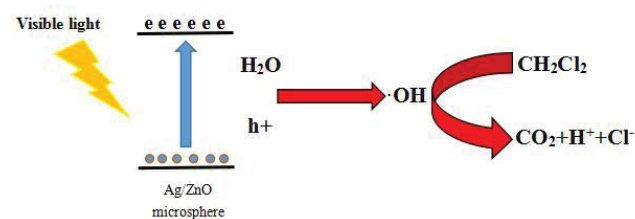


Fig. 7. Possible photocatalytic degradation mechanism of CH₂Cl₂ under visible light irradiation.

1.54 × 10⁻¹⁵ mol L⁻¹ in the composite microspheres prepared by soaking with 0.05 M Ag photocatalyst. The results of LC suggested that in the photocatalytic reaction, CH₂Cl₂ was dechlorinated into carbon dioxide and hydrogen chloride.

Acknowledgments

The present work was supported by the National Key Research and Development Program of China (2019YFC0408501), Project of Natural Science Foundation of Anhui Province (2008085QE243), and Natural Science Research Project of Universities in Anhui Province (KJ2019A0582). All authors here express their deep thanks.

References

- [1] M.Y. Wang, X.H. Zhang, Y. L. Chen, A. Zhang, Estimation of the desorption energy of dichloromethane and water in MIL-53 by DSC and ab-initio calculations, *Sci. China Chem.*, 59 (2016) 398–404.
- [2] S. Kumagai, Two offset printing workers with cholangiocarcinoma, *J. Occup. Health*, 56 (2014) 164–168.
- [3] B. Pavoni, D. Drusian, A. Giacometti, M. Zanette, Assessment of organic chlorinated compound removal from aqueous matrices by adsorption on activated carbon, *Water Res.*, 40 (2006) 3571–3579.
- [4] C. Wen, B.A. Bassig, R. Vermeulen, V.J. Seow, W. Hu, M.P. Purdue, H. Huang, N. Rothman, Q. Lan, A review of human exposure to dichloromethane, perchloroethylene and carbon tetrachloride in China, *Ann. Epidemiol.*, 24 (2014) 688–688, doi: 10.1016/j.annepidem.2014.06.034.
- [5] T.A. Saleh, K.R. Alhooshani, M.S.A. Abdelbassit, Evaluation of AC/ZnO composite for sorption of dichloromethane, trichloromethane and carbon tetrachloride: kinetics and isotherms, *J. Taiwan Inst. Chem. Eng.*, 55 (2015) 159–169.
- [6] K.P. Ramaiah, D. Satyasri, S. Sridhar, A. Krishnaiah, Removal of hazardous chlorinated VOCs from aqueous solutions using novel ZSM-5 loaded PDMS/PVDF composite membrane consisting of three hydrophobic layers, *J. Hazard. Mater.*, 261 (2013) 362–371.
- [7] X. Liang, P. Wang, M. Li, Q. Zhang, Z. Wang, Y. Dai, X. Zhang, Y. Liu, M.-H. Whangbo, B. Huang, Adsorption of gaseous ethylene via induced polarization on plasmonic photocatalyst Ag/AgCl/TiO₂ and subsequent photodegradation, *Appl. Catal., B*, 220 (2018) 356–361.
- [8] W. Cui, J. Li, F. Dong, Y. Sun, G. Jiang, W. Cen, S.C. Lee, Z. Wu, Highly efficient performance and conversion pathway of photocatalytic NO oxidation on SrO-clusters@amorphous carbon nitride, *Environ. Sci. Technol.*, 51 (2017) 10682–10690.
- [9] S. Wang, P. Kuang, B. Cheng, J. Yu, C. Jiang, ZnO hierarchical microsphere for enhanced photocatalytic activity, *J. Alloys Compd.*, 741 (2018) 622–632.
- [10] M.B. Tahir, M. Sagir, N. Abas, Enhanced photocatalytic performance of CdO-WO₃ composite for hydrogen production, *Int. J. Hydrogen Energy*, 44 (2019) 24690–24697.
- [11] J.H. Sun, S.Y. Dong, Y.K. Wang, S.P. Sun, Preparation and photocatalytic property of a novel dumbbell-shaped ZnO

- microcrystal photocatalyst, *J. Hazard. Mater.*, 172 (2009) 1520–1526.
- [12] B. Chai, X. Wang, S.Q. Cheng, H. Zhou, F. Zhang, One-pot triethanolamine-assisted hydrothermal synthesis of Ag/ZnO heterostructure microspheres with enhanced photocatalytic activity, *Ceram. Int.*, 40 (2014) 429–435.
- [13] F. Li, J.F. Wu, Q.H. Qin, Z. Li, X.T. Huang, A facile method to prepare monodispersed ZnO-Ag core-shell microspheres, *Superlattices Microstruct.*, 47 (2010) 232–240.
- [14] Y.G. Xu, H. Xu, H.M. Li, J.X. Xia, C.T. Liu, L. Liu, Enhanced photocatalytic activity of new photocatalyst Ag/AgCl/ZnO, *J. Alloys Compd.*, 509 (2011) 3286–3292.
- [15] Y. Peng, S.C. Qin, W.S. Wang, A.W. Xu, Fabrication of porous Cd-doped ZnO nanorods with enhanced photocatalytic activity and stability, *CrystEngComm*, 15 (2013) 6518–6525.
- [16] X.H. Huang, J.B. Wu, Y. Lin, R.Q. Guo, W.W. Zhong, Ag decorated hierarchical structured ZnO microspheres and their enhanced electrochemical performance for lithium ion batteries, *Int. J. Electrochem. Sci.*, 9 (2014) 6707–6716.
- [17] Q. Deng, H. Tang, G. Liu, X.P. Song, G.P. Xu, Q. Li, D.H.L. Ng, G.Z. Wang, The fabrication and photocatalytic performances of flower-like Ag nanoparticles/ZnO nanosheets-assembled microspheres, *Appl. Surf. Sci.*, 331 (2015) 50–57.
- [18] H.R. Liu, Y.C. Hu, Z.X. Zhang, X.G. Liu, H.S. Jia, B.S. Xu, Synthesis of spherical Ag/ZnO heterostructural composites with excellent photocatalytic activity under visible light and UV irradiation, *Appl. Surf. Sci.*, 355 (2015) 644–652.
- [19] H. Zangeneh, A.A. Zinatizadeh, S. Zinadini, M. Feyzi, E. Rafiee, D.W. Bahnemann, A novel L-Histidine (C, N) codoped-TiO₂-CdS nanocomposite for efficient visible photo-degradation of recalcitrant compounds from wastewater, *J. Hazard. Mater.*, 369 (2019) 384–397.
- [20] T.M. Bilal, M. Sagir, Carbon nanodots and rare metals (RM = La, Gd, Er) doped tungsten oxide nanostructures for photocatalytic dyes degradation and hydrogen production, *Sep. Purif. Technol.*, 209 (2018) 94–102.
- [21] X.H. Guo, J.Q. Ma, H.G. Ge, Preparation, characterization, and photocatalytic performance of pear-shaped ZnO/Ag core-shell submicrospheres, *J. Phys. Chem. Solids*, 74 (2013) 784–788.
- [22] S.S. Patil, R.H. Patil, S.B. Kale, M.S. Tamboli, J.D. Ambekar, W.N. Gade, S.S. Kolekar, B.B. Kale, Nanostructured microspheres of silver@zinc oxide: an excellent impeder of bacterial growth and biofilm, *J. Nanopart. Res.*, 16 (2014) 1–11.
- [23] J.W. Tringe, H.W. Levie, S.K. McCall, N.E. Testlich, M.A. Wall, C.A. Orme, M.J. Matthews, Enhanced Raman scattering and nonlinear conductivity in Ag-doped hollow ZnO microspheres, *Appl. Phys. A*, 109 (2012) 15–23.
- [24] H.Y. Wu, W.J. Jian, H.F. Dang, X.F. Zha, J.H. Li, Hierarchical Ag-ZnO microspheres with enhanced photocatalytic degradation activities, *Pol. J. Environ. Stud.*, 26 (2017) 871–880.
- [25] P. Fageria, S. Gangopadhyay, S. Pande, Synthesis of ZnO/Au and ZnO/Ag nanoparticles and their photocatalytic application using UV and visible light, *RSC Adv.*, 4 (2014) 24962–24972.
- [26] W.W. Lu, S.Y. Gao, J.J. Wang, One-pot synthesis of Ag/ZnO self-assembled 3D hollow microspheres with enhanced photocatalytic performance, *J. Phys. Chem. C*, 112 (2008) 16792–16800.
- [27] D.D. Lin, H. Wu, R. Zhang, W. Pan, Enhanced photocatalysis of electrospun AgZnO heterostructured nanofibers, *Chem. Mater.*, 21 (2009) 3479–3484.
- [28] G. Zhang, X. Shen, Y. Yang, Facile synthesis of monodisperse porous ZnO spheres by a soluble starch-assisted method and their photocatalytic activity, *J. Phys. Chem. C*, 115 (2011) 7145–7152.
- [29] J. Rodriguez-Fernandez, A.M. Funston, J. Perez-Juste, R.A. Alvarez-Puebla, L.M. Liz-Marzan, P. Mulvaney, The effect of surface roughness on the plasmonic response of individual sub-micron gold spheres, *Phys. Chem. Chem. Phys.*, 11 (2009) 5909–5914.
- [30] Y. Cheng, L. An, J. Lan, F. Gao, R.Q. Tan, X.M. Li, G.H. Wang, Facile synthesis of pompon-like ZnO-Ag nanocomposites and their enhanced photocatalytic performance, *Mater. Res. Bull.*, 48 (2013) 4287–4293.
- [31] Y.M. Liang, N. Guo, L.L. Li, R.Q. Li, G.J. Ji, S.C. Gan, Fabrication of porous 3D flower-like Ag/ZnO heterostructure composites with enhanced photocatalytic performance, *Appl. Surf. Sci.*, 332 (2015) 32–39.
- [32] N.R. Khalid, M. Liaqat, M.B. Tahir, G. Nabi, T. Iqbal, N.A. Niaz, The role of graphene and europium on TiO₂ performance for photocatalytic hydrogen evolution, *Ceram. Int.*, 44 (2018) 546–549.
- [33] Z.B. Xu, J.P. Yan, L. Wu, Study on preparation and photocatalytic activity of ZnO hollow spheres, *J. Synth. Cryst.*, 41 (2012) 1722–1725 (in Chinese).
- [34] G.V. Buxton, C.L. Greenstock, W.P. Helman, A.B. Ross, Critical review of rate constants for reactions of hydrated electrons, hydrogen atoms and hydroxyl radicals ([•]OH/[•]OH) in aqueous solution, *J. Phys. Chem. Ref. Data*, 17 (1988) 513–886.
- [35] C. Ren, B. Yang, M. Wu, J. Xu, Z. Fu, Y. Lv, T. Guo, Y. Zhao, C. Zhu, Synthesis of Ag/ZnO nanorods array with enhanced photocatalytic performance, *J. Hazard. Mater.*, 182 (2010) 123–129.
- [36] L.Z. Sun, S.Z. Zhao, Z.L. Gao, Z.Q. Cheng, Controllable synthesis of Ag decorated ZnO nanofibers for enhanced photocatalysis, *Chem. J. Chin. Univ.*, 38 (2017) 907–914.
- [37] H.J. Jung, R. Koutavarapu, S. Lee, J.H. Kim, H.C. Choi, M.Y. Choi, Enhanced photocatalytic degradation of lindane using metal-semiconductor Zn@ZnO and ZnO/Ag nanostructures, *J. Environ. Sci.*, 74 (2018) 107–115.
- [38] C. Yu, D.B. Zeng, Q.Z. Fan, K. Yang, J.L. Zeng, L.F. Wei, J.H. Yi, H.B. Ji, The distinct role of boron doping in Sn₃O₄ microspheres for synergistic removal of phenols and Cr(VI) in simulated wastewater, *Environ. Sci. Nano*, 7 (2020) 286–303.
- [39] D.B. Zeng, C.L. Yu, Q.Z. Fan, J.L. Zeng, L.F. Wei, Z.S. Li, K. Yang, H.B. Ji, Theoretical and experimental research of novel fluorine doped hierarchical Sn₃O₄ microspheres with excellent photocatalytic performance for removal of Cr(VI) and organic pollutants, *Chem. Eng. J.*, 391 (2020) 123–607.
- [40] M.B. Tahir, G. Nabi, N.R. Khalid, M. Rafique, Role of europium on WO₃ performance under visible-light for photocatalytic activity, *Ceram. Int.*, 44 (2018) 5705–5709.
- [41] K.Z. Qi, B. Cheng, J.G. Yu, W.K. Ho, Review on the improvement of the photocatalytic and antibacterial activities of ZnO, *J. Alloys Compd.*, 727 (2017) 792–820.
- [42] C. Gu, C. Cheng, H. Huang, T. Wong, N. Wang, T.Y. Zhang, Growth and photocatalytic activity of dendrite-like ZnO@Ag heterostructure nanocrystals, *Cryst. Growth Des.*, 9 (2009) 3278–3285.
- [43] J. Liu, Y. Liu, N.Y. Liu, Y.Z. Han, X. Zhang, H. Huang, Y. Lifshitz, S.T. Lee, J. Zhong, Z.H. Kang, Metal-free efficient photocatalyst for stable visible water splitting via a two-electron pathway, *Science*, 347 (2015) 970–974.
- [44] H. Kawaguchi, Steady-state concentrations of hydroxyl radical in titanium dioxide aqueous suspensions, *Chemosphere*, 22 (1991) 1003–1009.
- [45] M.D. Bhatt, G. Lee, J.S. Lee, Screening of oxygen-reduction-reaction-efficient electrocatalysts based on Ag-M (M = 3d, 4d, and 5d transition metals) nanoalloys: a density functional theory study, *Energy Fuel*, 31 (2017) 1874–1881.
- [46] Y. Lai, M. Meng, Y. Yu, One-step synthesis, characterizations and mechanistic study of nanosheets-constructed fluffy ZnO and Ag/ZnO spheres used for Rhodamine B photodegradation, *Appl. Catal., B*, 100 (2010) 491–501.